Received: 7 January 2019 | Revised and accepted: 16 March 2019

DOI: 10.1002/jccs.201900010

JOURNAL OF THE CHINESE CHEMICAL SOCIETY

ARTICLE

Synthesis, characterization, and anticancer activity of some azole-heterocyclic complexes with gold(III), palladium(II), nickel(II), and copper(II) metal ions

Zahraa M. Abdnoor | Ammar J. Alabdali

Department of Chemistry, College of Sciences, Al-Nahrain University, Baghdad, Iraq

Correspondence
Ammar J. Alabdali, Department of Chemistry, College of Sciences, Al-Nahrain University, Baghdad, Iraq.
Email: ammarjehad_2004@yahoo.com

Four new complexes of Au(III), Pd(II), Ni(II), and Cu(II) ions were synthesized, derived from a novel heterocyclic ligand (L) that has both triazole and tetrazole rings. The ligand synthesis was through successive steps to achieve both heterocyclic rings. The synthesized compounds were characterized using conventional techniques like infrared, ultra violet—visible and proton/carbon nuclear magnetic resonance spectroscopy, metal and thermal analyses, and molar conductivity. All complexes were suggested to have square planar geometry, gold, nickel, and palladium complexes were salts while copper neutral complexes have the chemical formulas; $[AuL_2]Cl.2H_2O$, $[PdL_2]Cl_2.2H_2O$, $[NiL_2]Cl_2.2H_2O$, and $[CuL_2]$. The cytotoxic effect was studied on breast cancer cell line (MCF-7 cell line) at different concentrations by using the 3-(4,5-dimethylthiazol-2-yl)-2,5-diphenyltetrazolium bromide assay method, for the ligand (L) and complexes. The results showed that gold(III) and nickel(II) complexes have the highest cytotoxicity among all compounds against cancer cell lines.

KEYWORDS

anticancer compounds, cell viability assay, cupper(II) complexes, gold (III), nickel(II), palladium(II), tetrazole derivatives,1,2,4-triazole

1 | INTRODUCTION

Cancer is a diverse group of diseases identified by the production and prevalence of abnormal cells, and is a major global problem.[1] Therefore, the discovery and development of new effective and selective anticancer drugs are of high importance in modern cancer research. Nitrogen-based heterocycles such as triazoles and tetrazoles are five membered ring heterocyclic compounds and they have earned great interest in medicinal chemistry as anticancer agents.[2,3] 1,2,4-triazole, for example, has been found to inhibit the growth of various cancers including lung,[4] colon,[5] renal, ovarian, leukemia prostate, and breast.[6] Tetrazole and its derivatives, on the other hand, exhibit a wide variety of biological properties including antibacterial,[7] antimicrobial,[8] anti-inflammatory,[9] antifungal,[10] antiviral,[11] antinociceptive,[12] analgesic,[13] cyclo-oxygenase inhibition,[14] and anticancer activities.[3] Tetrazole derivatives exhibited anticancer activity against Hep G2,[3,15] A 549, DU 145,[15] and MCF-7 cell lines.[16,17]

Metal complexes of substituted tetrazoles have been of interest lately to pharmaceutical investigators because of their ability to act as antitumor agents[18] These complexes can exhibit several modes of coordination. They may bond as unidentate form through the N1 or the N2 position of the tetrazole ring or they can act as a bidentate ligand.[19]

Many coordinated compounds (metal-based drugs) were used as chemotherapeutic agents to treat cancers.[20] The anticancer activity of cisplatin (cis-diamminedichloroplatinum(II)) was discovered by Barnett Rosenberg and coworkers in 1969,[21] which has been used extensively for different types of neoplasms including head, neck, ovarian, bladder, endometrial, cervical, testicular, osteogenic

sarcoma, and lung cancers.[22] After using cisplatin as an antitumor agent successfully, many other complexes containing platinum or other metals such as, vanadium,[23] ruthenium[23], copper,[23] iron,[24] cobalt,[25] palladium,[26] rhodium,[27] zinc,[27] and nickel have been proposed with selectivity and cytotoxicity toward tumor cells.[27]

Gold(III) complexes with chelating N-donor ligands are the first gold(III) complexes examined for anticancer applications,[28] in vitro pharmacological studies point out that some of these novel gold(III) complexes are highly cytotoxic toward cultured human tumor cell lines,[29] pyridine-based complexes were tested in vitro against a panel of cancer cell lines and HeLa cancer cells.[30–32] Palladium(II), nickel(II), and copper(II) complexes also were very promising candidates for anticancer therapy, this idea was supported by a number of research articles relating the synthesis and cytotoxic activities of numerous Pd(II),[33,34] Ni(II),[35–37] and Cu(II) complexes.[38]

In this study, we report the preparation and characterization of square planar gold(III), palladium(II), nickel(II), and copper(II) complexes with a tetrazole derivative ligand, namely 4-{[(3,4 dimethoxyphenyl) (1*H*-tetrazol-5-yl)methyl]amino}-5-phenyl-4*H*-1,2,4-triazole-3-thiol compound (**6**), as shown in Scheme.1. Additionally, the synthesized metal complexes and the ligand were screened for studying their potential in vitro cytotoxicity against breast cancer (MCF7) cell lines.

2 | EXPERIMENTAL

2.1 | Materials and instruments

All the reagents, starting materials as well as solvents were purchased commercially and used without any further purification. Melting points were determined by the open capillary method using hot stage Gallenkamp melting point apparatus and was uncorrected.^{1}HNMR and ^{13}CNMR spectra were recorded on a Bruker spectrophotometer model ultra shield at 300 MHz in DMSO-*d*6 solution with the Tetramethylsilane as internal standard. Infrared spectra were recorded using a Fourier transform-infrared (FT-IR).8300 Shimadzu spectrophotometer and a Bruker alpha FT-IR Spectrophotometer in the (4,000–400) cm^{-1} range. The

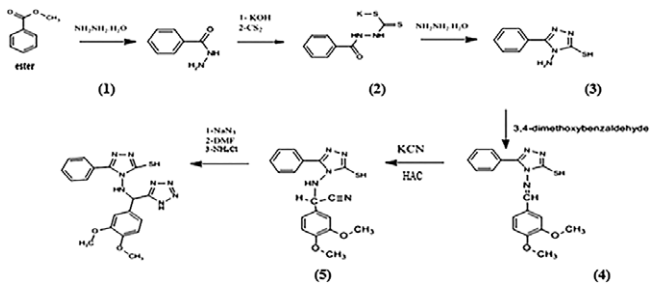

SCHEME 1 Synthesis steps to produce compound (**6**)

Ultraviolet-Visible spectra were recorded on a Shimadzu UV–Vis. 1600A Ultra Violate Spectrophotometer in the range (200–1,100) nm. TGA was performed using a Linseis STA PT-1000 Thermo Gravimetric Analyzer. Conductivity measurements were obtained with corning conductivity meter 220 using absolute ethanol as a solvent with 10^{-3} M concentration. The metal content of the complexes was measured using the flame-atomic absorption technique by nov AA 350.

2.2 | Synthesis

2.2.1 | Synthesis of benzoic acid hydrazide (1)

A volume of 15 mL (0.12 mol, 16.33 g) of methyl benzoate was refluxed for 1 hr with 5.8 mL hydrazine hydrate (0.12 mol, 6 g), then 20 mL absolute ethanol was added and continued to reflux for 4 hr. The solution produced was cooled and the white crystals were collected then recrystallized from ethanol.

2.2.2 | Synthesis of 4-amino-5-phenyl-4H-1,2,4-triazole-3-thiol (3)

Compound **1** (0.01 mol, 1.52 g) was added to potassium hydroxide (0.03 mol, 1.68 g) dissolved in 25 mL abs. ethanol, the mixture was stirred, then 6 mL carbon disulfide CS_2 (0.05 mol) was added dropwise to the mixture and continued stirring for 18 hr, to form salt (**2**), then excess CS_2 was evaporated, and 10 mL hydrazine hydrate was added to salt (**2**). The solution was refluxed until hydrogen sulfide (H_2S) evolved (tested by lead acetate paper), the mixture was cooled at room temperature, and diluted by 20 mL cold water then acidified by concentrated hydrochloric acid. A white precipitate was filtered and dried.

2.2.3 | Synthesis of (3,4-dimethoxyphenyl) [(3-phenyl-5-sulfanyl-4H-1,2,4-triazol-4-yl) amino]acetonitrile (5)

The compound **3** (0.01 mol, 1.92 g) was refluxed for 1 hr with veratrumaldehyd (0.01 mol,1.66 g), which was mixed in 12 mL glacial acetic acid to form imine, compound (**4**) with yellow precipitates. Potassium cyanide (0.02 mol, 1.3 g) was added carefully to the imine and continued to reflux for 24 hr. The mixture was poured onto crushed ice and made slightly alkaline with the addition of ammonia solution (tested by red litmus paper). The pale yellow precipitate α-amino nitrile was filtered, washed with water, and dried. The presence of the nitrile group was indicated by heating a small amount of α-amino nitrile with 10% sodium hydroxide solution, the liberation of ammonia was detected by wet red litmus paper.

2.2.4 | Synthesis of 4-{[(3,4-dimethoxyphenyl) (1H-tetrazol-5-yl) methyl]amino}-5-phenyl-4H-1,2,4-triazole-3-thiol (6)

α-amino nitrile compound (**5**) (0.005 mol,1.84 g) was refluxed with sodium azide (0.01 mol, 0.65 g) in 10 mL Dimethylformamide for 24 hr in the presence of a small amount of ammonium chloride. The brown solution was dried and our desired product (compound **6**) was collected and purified by cold recrystallization.

2.2.5 | Synthesis of metal ion complexes

A volume of 0.1 mol of metal ion salt (chloroauric acid, palladium chloride anhydrous, nickel chloride hexahydrate or copper chloride dihydrate) dissolved in 5 mL absolute ethanol was added dropwise to an ethanolic solution of compound **6** (0.2 mol) and refluxed for 3 hr. The mixture was filtered after cooling to room temperature and dried, then collected and stored in desiccators

2.3 | MTT assay method

The cytotoxicity profiles of L and complexes were assessed using the 3-[4,5- dimethylthiazol-2-yl]-2,5-diphenyltetrazolium bromide (MTT) microculture tetrazolium viability assay. Tumor cells (1×10^4–1×10^6 cells/mL) were grown in 96 flat well microtiter plates, in a final volume of 200 μL complete culture medium per each well. The microplate was covered by sterilized parafilm and shaken gently. The plates were incubated at 37°C, 5% CO_2 for 24 hr. After incubation, the medium was removed and twofold serial dilutions of the desired compound (12.5, 25, 50, 100, 200, and 400) μg/mL were added to the wells. Triplicates were used per each concentration as well as the controls (cells treated with serum free medium). Plates were incubated at 37°C, 5% CO_2 for selected exposure time (24 hr). After exposure, 10 μL of the MTT solution was added to each well. Plates were further incubated at 37°C, 5% CO_2 for 4 hr. The media were carefully removed and 100 μL of solubilization solution was added per each well for 5 min. The absorbance was determined by using an ELISA reader at a wavelength of 575 nm. The data of optical density were subjected to statistical analysis to calculate the concentration of compounds required to cause 50% reduction in cell viability for each cell line.

The cytotoxicity of samples on cancer cells was expressed as IC_{50} values, the reduction of the absorbance of treated cells by 50% with respect to untreated cells by the drug concentration.

3 | RESULTS AND DISCUSSION

Compounds (1-6) were synthesized as shown in Scheme 1. The physical properties of these compounds are listed in Table 1 and the physical properties of synthesized complexes with metal content are listed in Table 2.

3.1 | Infrared spectroscopy

The infrared spectra and absorption bands of all synthesized organic compounds (**1**–**6**) were described and showed with some characteristic peaks in Table 3.

3.2 | Benzoic acid hydrazide compound (1)

The infrared spectrum of compound (**1**) showed absorption bands of functional groups in a good agreement with ranges reported in previous works ,[39,40] the peaks appearing at (ν 3,300 and ν 3,200) cm^{-1} could be of N-H stretching bands asymmetric and symmetric, respectively. The carbonyl group stretching of amide appeared at 1,655 cm^{-1}. The peaks at 1,568 and 1,616 cm^{-1} represented stretching bands of the νC=C aromatic group and bending of the amide N-H group, respectively.

3.3 | 4-amino-5-phenyl-4H-1,2,4-triazole-3-thiol compound (3)

The infrared spectrum of compound (**3**) showed two stretching bands at (3,300 and 3,200) cm^{-1} for asymmetric and symmetric stretching of the N-H group. The SH-group showed two stretching bands at 2,761.9 and 1,072 cm^{-1} for S-H and C=S, respectively, due to the thione-thiol tautomerism. The other characteristic bands of νC=C stretching of

TABLE 1 The physical properties of organic synthesized compounds

Compound no.	Chemical formula	Molecular weight (g $mole^{-1}$)	Melting point (°C)	Color	Yield percentage
1	$C_7H_8N_2O$	136.2	109–111	White	58
2	$C_8H_7KN_2OS_2$	250.4	—	Yellow	—
3	$C_8H_8N_4S$	192.2	178–180	White	82
4	$C_{17}H_{16}N_4O_2S$	340.4	—	Yellow	—
5	$C_{18}H_{17}N_5O_2S$	367.4	143–145	Pale yellow	73
6 (L)	$C_{18}H_{18}N_8O_2S$	410.5	139–141	Brown	62

TABLE 2 The physical properties and metal contents of the synthesized complexes

Complexes	Chemical formula	Molecular weight (g/mol)	Melting point (°C)	Color	Yield percentage	Metal percentage	
						Calculated	Founded
Au(III)	$C_{36}H_{38}N_{16}S_2O_6ClAu$	1,086.416	148–150	Reddish-orange	45	18.13	18.09
Ni(II)	$C_{36}H_{40}N_{16}S_2O_6Cl_2Ni$	985.59	$140_{dec.}$	Orange	60	5.95	6.06
Pd(II)	$C_{36}H_{40}N_{16}S_2O_6Cl_2Pd$	1,033.32	$156_{dec.}$	Green	40	10.29	11.42
Cu(II)	$C_{36}H_{34}N_{16}S_2O_4Cu$	881.55	148–150	Brown	55	7.21	8.09

TABLE 3 The most important absorption bands of the synthesized organic compounds

Compound	*ν* (N-H), cm^{-1}	*ν* (C-H) cm^{-1}		*ν* (S-H), cm^{-1}	*ν* (C=N), cm^{-1}	*δ* (N-H), cm^{-1}	*ν* (C=C), cm^{-1}	*ν* (C-O), cm^{-1}	*ν* (C=S), cm^{-1}	Other bands, cm^{-1}
		Arom.	Aliph.							
1	3,300	3,018	—	—	—	1,616	1,568	—	—	*ν* (C=O)
	3,200									1,655
3	3,300	3,130	—	2,762	1,639	1,606	1,533	—	1,072	—
	3,260									
5	3,300	3,000	2,955	2,410	1,640	1,606	1,571	1,271	—	*ν* (C≡N)
			2,820							2,278
6	3,298	3,000	2,931	—_	Masked	1,601	1,510	1,269	1,142	*ν* (N=N)
			2,837							1,461

Aliph.: aliphatic; Arom.: aromatic.

aromatic, *ν*C=N stretching, and δN-H bending appeared at 1,533, 1,639, and 1,606 cm^{-1}, respectively.[40,41]

3.4 | (3,4-dimethoxyphenyl([(3-phenyl-5-sulfanyl-4H-1,2,4-triazol-4-yl)amino] acetonitrile compound (5)

The infrared spectrum of compound (**5**) showed a new characteristic band at 2,277 cm^{-1}, which could be attributed to the *ν* C≡N group, which normally accrues in the (2,280 –2,200) cm^{-1} range,[42,43] the presence of the nitrile group indicated the formation of α-amino nitrile compound (**5**), which was supported by the chemical test as shown in the experimental part. Furthermore, the disappearance of the amino group ($-NH_2$) and the appearance of the NH-group at 3,300 cm^{-1} as a single peak in addition to the methoxy group ($-OCH_3$) of aldehyde at 1,271 cm^{-1} for *ν*C-O stretching was considered another evidence for the formation of compound (**5**).

3.5 | 4-{[(3,4-dimethoxyphenyl)(1H-tetrazol-5-yl)methyl]amino}-5-phenyl-4H-1,2,4-triazole-3-thiol (6)

The infrared spectrum of compound (**6**) showed the disappearance of the nitrile group (C≡N) and the appearance of the *ν*N=N band at 1,461 cm^{-1} of the tetrazole group.[42]

3.6 | Nuclear magnetic resonance spectroscopy

Nuclear magnetic resonance spectroscopy was used for the characterization of the newly synthesized compounds, α-amino nitrile compound (**5**) and tetrazole compound (**6**). ^{1}HNMR and ^{13}CNMR spectra were used to confirm the final structure of compounds.

3.7 | ^{1}HNMR and ^{13}CNMR spectra of compound (5)

The ^{1}HNMR spectrum of compound (**5**), Figure 1, showed a singlet signal at 14.18 ppm for the S-H group. A doublet signal at 7.06 ppm appeared for N-H of the amine group. The C-H signals of aliphatic carbon that was bonded with nitrile group appear at 5.5 ppm and for the methoxy group $O-CH_3$ appeared as a singlet at (3.8 and 3.81) ppm, while for the aromatic group appeared as a multiplet in the range (8.2–7.5) ppm.[44] Furthermore, the ^{13}CNMR spectrum of compound (**5**), Figure 2, showed a signal at 124.78 ppm for the (C≡N) group.[45] The aromatic carbon signals of two phenyl rings appeared at (127.18, 123.9, 112.15, and 111.97) ppm, while the aliphatic carbon signals at (153.47, 167.24, and 56.1) ppm for (Ph-C), (C-SH), and ($O-CH_3$) groups, respectively.[46]

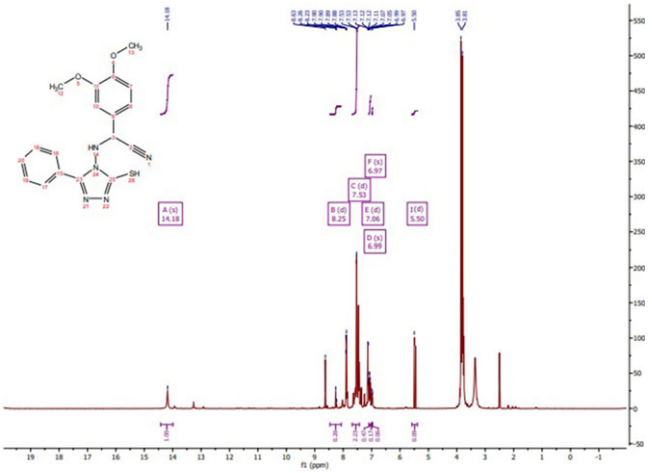

FIGURE 1 ^{1}HNMR spectra of compound (**5**)

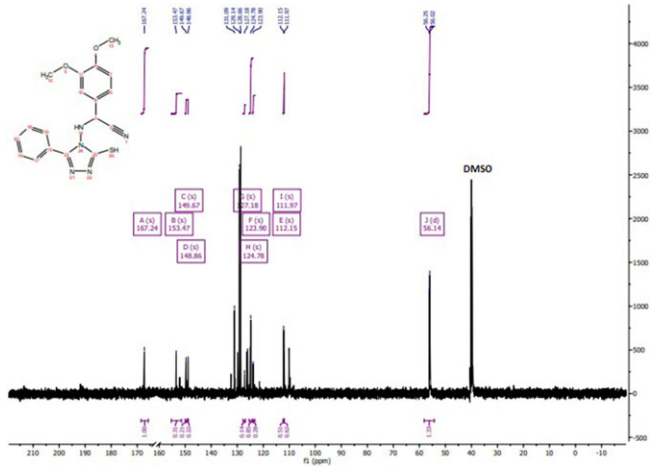

FIGURE 2 ^{13}CNMR spectra of compound (**5**)

3.8 | ^{1}HNMR and ^{13}CNMR spectra of compound (6)

The ^{1}HNMR spectrum of compound (**6**), Figure 3, showed approximate disappearance of the S-H signal due to the stabilized tautomerism thion form (C=S). A broad signal at a low field nearly 14 ppm could be attributed to the SH-group similar to compound (**5**). The significant appearance of the SH-group in compound (**5**) due to the enhancement by nitrile group due to forming hydrogen bonding and absence of steric factor that presented in compound (**6**) by bulky tetrazole group and sp^2 hybridization (nonlinear geometry). The multiple signals at (8.6–7.47) ppm indicate the C-H presence of phenyls groups. Doublet signal at 7.07 ppm is attributed to the NH-group bonded to the triazole ring and a singlet signal at 6.45 ppm attributed to N-H of the tetrazole ring.[44] The two singlet signals at 3.83 ppm and 3.34 ppm could be attributed to C-H of the OCH_3-group.

Furthermore, the ^{13}CNMR spectrum of compound (**6**), Figure 4, show the disappearance of the signal of the

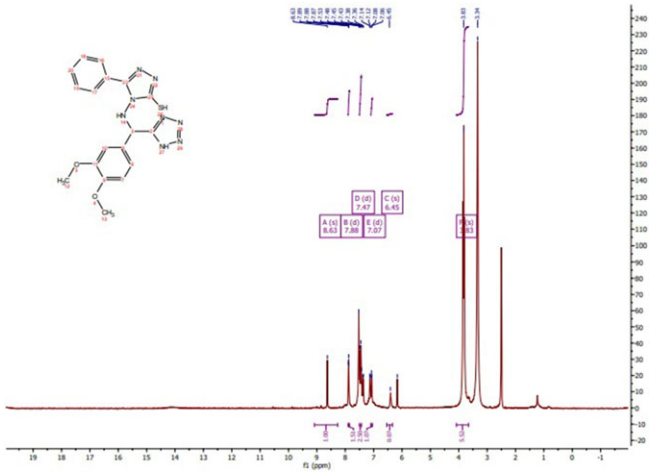

FIGURE 3 ^{1}HNMR spectra of compound (**6**)

(C≡N)-group at 124.7 ppm and appearance of a signal at 160.8 ppm, attributed to carbon in the tetrazole ring.[46] The signals at (130.6–111.8) ppm indicate carbons of phenyl rings. The two signals at 167.2 ppm and 55.8 ppm could be attributed to C=S and CH_3-O groups, respectively.

3.9 | Infrared spectroscopy of metal complexes

The infrared spectra of the prepared complexes were compared with those of the free ligand compound (**6**)to determine the coordination sites that may get involved in chelation. The absorption bands of complexes are shown in Table 4.

The infrared spectrum of the Au(III) complex showed that the N-H bending band was shifted to a low frequency (red shift) by 14 cm^{-1}. The disappearance of the N-H absorption band of the tetrazole group indicated that the complexation occurs through nitrogen of the tetrazole ring losing a proton. The slightly broad band at 3,523 cm^{-1} indicated the presence of lattice water molecules in the compound.[42]

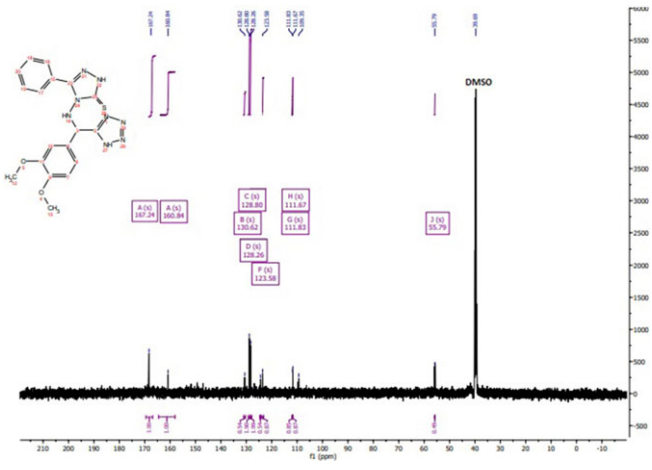

FIGURE 4 ^{13}CNMR spectra of compound (**6**)

TABLE 4 The most important absorption bands of the synthesized metal complexes

Complexes	ν (O-H), cm^{-1}, H_2O latt.	ν (C-H), cm^{-1}, Aliph.	ν (S-H), cm^{-1}	δ(N-H), cm^{-1}	ν(N=N), cm^{-1}
Au(III)	≈3,320	2,926	2,612	1,589.8	1,455
		2,846			
Ni(II)	3,472	2,928	≈2,430	1,595.7	1,450
		2,835.8			
Pd(II)	3,327.8	2,930.8	2,608	1,593	1,459
		2,835			
Cu(II)	—	2,909	≈2,621	1,593	1,449
		2,837			

Aliph.: aliphatic; latt.: lattice.

Infrared spectrum of the Ni(II) complex illustrated that the N-H stretching band appears at 3,296.8 cm^{-1} while N-H bending was shifted to a low frequency by 5 cm^{-1} due to complexation. The absorption band at 3,472 cm^{-1} indicated the presence of the νO-H lattice water molecules.[42] The M-N absorption band appeared at 615 cm^{-1} for Ni-N.[47]

The infrared spectrum of the Pd(II) complex showed the NH-group bending was shifted to a low frequency (red shift) by 8 cm^{-1} due to complexation through nitrogen, the absorption band at 3,327.8 cm^{-1} indicates the presence νO-H lattice water molecules.[42]

For the Cu(II) complex, the infrared spectrum shows a shift of the N-H bending band to low frequency by 8 cm^{-1} due to complexation through nitrogen losing a proton. The M-N absorption band appeared at 516 cm^{-1} for Cu-N.[47]

4 | THERMAL STUDIES

Thermo gravimetric analysis was carried out for the prepared metal complexes from 0 to 600°C in atmospheric air. The decomposition temperature, mass loss percentage, and the residue percent of the complexes are given in Table 5.

4.1 | Ultraviolet–visible spectroscopy

The Ultraviolet–visible electronic spectra of the synthesized complexes and ligand (L) were recorded in the range of (250–1,100) nm at room temperature using DMSO solvent and a concentration of 10^{-3} M. The electronic spectrum of the ligand (L) shows two peaks; the first at ~310 nm due to the n → π* transition of nonbonding electrons, and the second at 283 nm that can be assigned to π → π* transition of the benzene and aromatic rings.[48]

The electronic spectrum of the Au(III) complex showed one peak at~341 nm, which could be assigned to $^1A_{1g} \rightarrow {}^1B_{1g}$ transition in square planer geometry and another peak at ~312 nm, which could be assigned to the ligand field .[49] As the gold ion has a large size, it is in the third transition series and has a high oxidation state, the complexes have a high crystal field effect. Thus, the spectrum of such ion was characterized by a charge transfer band that dominates the ligand field transition.[49,50] The Ni(II) complex showed d-d electronic transition band at 895 nm, which can be assigned to $^1A_g \rightarrow {}^1B_{1g}$ in square planer geometry.[51,52] The Pd(II) complex showed transition bands at 690 nm and at 311 nm, which can be assigned to $^1A_{1g} \rightarrow {}^1A_{2g}$ and $^1A_{1g} \rightarrow {}^1E_g$.[53–55] The Cu(II) complex showed broad bands at

TABLE 5 Thermogravimetric analysis results for metal complexes

Complexes	TG range/°C	Mass loss%		Assignments
		Absolute	Calculated	
Au(III)	0–131.9	2.96	3.31	• $2H_2O$(lattice)
	131.9–390.2	49.45	48.95	• $2H_2S$, HCl, $2(OCH_3)_2Ph$, $2C_6H_5$
	390.2–540	26.71	26.88	• $2C_2N_3$, $2(CH–CHN_4)$
				• Au-N (residue)
Ni(II)	0–393.3	32.19	33	• $2H_2O$(lattice), $2H_2S$,Cl_2, $2C_6H_5$
	393.3–600	14.63	13	• $4CH_3O$
				• $C_{20}N_{16}O_4Ni$ (residue))
Pd(II)	0–110	3.53	3.8	• $2H_2O$ (lattice)
	110–353.9	33.61	31.6	• Cl_2, $2H_2S$, $2C_6H_5$
	353.9–600	30.06	29.6	• $2(OCH_3)_2Ph$
				• $C_8H_4N_{16}Pd$ (residue)
Cu(II)	0–337.9	24.40	25.11	• $2H_2S$, C_6H_5
	337.9–600	13.19	14.03	• $4CH_3O$
				• $C_{20}H_8N_{14}Cu$ (residue)

TABLE 6 Electronic spectra of the prepared complexes and ligands

Compound	Absorption (nm)	Assignment	Suggested geometry
6 (L)	~310, 283	$n \rightarrow \pi^*$, $\pi \rightarrow \pi^*$	—
Au(III)	~341, ~312	$^1A_{1g} \rightarrow {}^1B_{2g}$, $^1A_{1g} \rightarrow {}^1E_u$	Square planar
Ni(II)	895	$^1A_g \rightarrow {}^1B_{1g}$	Square planar
Pd(II)	690, 311	$^1A_{1g} \rightarrow {}^1A_{2g}$, $^1A_{1g} \rightarrow {}^1E_g$	Square planar
Cu(II)	810, 702	$^2B_1g \rightarrow {}^2A_1g$, $^2B_1g \rightarrow {}^2Eg$	Square planar

TABLE 7 Conductivity of the complexes in absolute ethanol

Complex	Conductivity (μs)	Property
Au(III)	35.2	Electrolyte
Ni(II)	63.3	Electrolyte
Pd(II)	72.8	Electrolyte
Cu(II)	20.3	Non-electrolyte

810 nm and 702 nm, which can be assigned to $^2B_1g \rightarrow {}^2A_1g$ and $^2B_1g \rightarrow {}^2Eg$ transitions, respectively, in square planer geometry.[56] Table 6 illustrates the electronic spectra of the synthesized complexes.

4.2 | Atomic absorption

Metal analysis of synthetic complexes is important for predicting the formula and final structure using atomic absorption spectroscopy. The calculated theoretical values are in a good agreement with the established experimental values, it can be clarified in Table 2.

4.3 | Molar conductivity

Molar conductance of the complexes was measured by using absolute ethanol as a solvent at 10^{-3} M. The synthesized complexes show 1:1 electrolytic form for the Au(III) complex and 1:2 electrolytic form for Ni(II) and Pd(II) complexes, while the Cu(II) complex showed non-electrolytic properties,[57,58] Table 7 shows the electrolytic behavior of each complex.

4.4 | Cytotoxic effect of the ligand and its complexes on MCF-7 cell line (MTT assay)

Normal cell line (WRL68) and cancer cell line (MCF-7) were treated with the synthesized compounds (L, Au(III), Pd(II), Ni(II), and Cu(II)) at various concentrations (400, 200, 100, 50, and 25)μg/mL, the results illustrated that all the tested compounds are active against the breast cancer (MCF7) cell line compared with the normal cell line (WRL68), furthermore they were significantly less toxic against the normal cell line.

The viability of the normal cell line WRL68 when treated with prepared compounds at different concentrations ranging from 400 μg/mL to 25 μg/mL decreased with increasing concentration, that is, an increase in toxicity. The results exhibited nontoxicity at lower concentrations (100, 50 and 25) μg/mL for all compound and less toxicity at high concentrations (400 and 200 μg/mL). The viability rate percentage of the complexes at 400 μg/mL were compared with viability rate of the ligand; clarifying that the Au(III) complex was less toxic than ligand (L) on the normal cell line, while Ni(II), Pd(II), and Cu(II) were almost equal to the ligand (Table 8).

The viability of MCF-7 breast cancer cell line for synthesized compounds at concentrations ranging from 400 to 25 μg/mL is illustrated in Table 9. The cell viability decreases with increasing concentration, that is, cytotoxicity increases. The viability of the prepared complexes at 400 μg/mL were compared with viability of the ligand (L), the results clarified that Au(III) and Ni(II) exhibited high cytotoxicity against the MCF-7 cancer cell line than ligand, while the Pd(II) and Cu(II) complexes showed lower cytotoxicity than the ligand (L). The half maximal inhibitory concentration (IC_{50}) of the prepared complexes in normal cell line WRL86 and cancer cell line MCF-7 is shown in Figure 5.

The antitumor activity results indicated that all the tested compounds are active against breast cancer (MCF7) cell line.

TABLE 8 Cytotoxicity effect of prepared compounds on the WRL68 normal cell line

Compound	Viability at different concentrations (μg/mL)					Growth inhibition (%)	IC_{50}(μg/mL)
	400	200	100	50	25		
Au(III)	63.7 ± 2.0	68.8 ± 0.8	94.2 ± 1.05	95.8 ± 0.2	95.3 ± 0.5	36.3	816
Ni(II)	74.8 ± 0.7	78.36 ± 1.8	90.9 ± 1.65	95.3 ± 0.3	94.9 ± 0.2	25.2	597
Pd(II)	74.7 ± 1.1	86.1 ± 1.8	93.8 ± 1.7	95.4 ± 0.3	95.9 ± 0.4	25.3	3,146
Cu(II)	73.0 ± 0.1	84.4 ± 0.1	94.2 ± 1.14	95.1 ± 0.3	94.8 ± 0.3	27.0	1,819
6 (L)	75.8 ± 1.2	84.2 ± 0.34	92.7 ± 1.09	96.0 ± 0.3	96.8 ± 0.2	24.2	1,374

TABLE 9 Cytotoxicity effect of prepared compounds on the MCF7 tumor cell line

Compound	Viability at different concentrations (μg/mL)					Growth inhibition (%)	IC_{50}(μg/mL)
	400	200	100	50	25		
Au(III)	39.5 ± 0.98	56.9 ± 2.4	68.1 ± 1.3	72.3 ± 0.7	94.8 ± 1.1	60.5	132.2
Ni(II)	37.3 ± 2.7	49.2 ± 0.9	72.4 ± 2.0	89.8 ± 1.5	95.6 ± 0.4	62.7	283.9
Pd(II)	55.8 ± 2.1	72.8 ± 0.9	87.7 ± 1.1	94.5 ± 1.5	95.6 ± 0.4	44.2	2,827
Cu(II)	67.5 ± 2.6	77.5 ± 0.9	89.1 ± 1.9	95.8 ± 0.2	95.3 ± 0.4	32.5	1,227
6 (L)	52.4 ± 2.5	68.3 ± 2.5	84.2 ± 1.8	93.1 ± 1.2	96.2 ± 0.3	47.6	783.2

By comparing between the synthesized metal complexes and the organic ligand (L), it is obvious that the organic heterocyclic ligand (L) showed moderate anticancer activity against the MCF7 cell line. While both Cu(II) and Pd(II) complexes exhibited lower anticancer activity, but Au(III) and Ni(II) complexes showed higher growth inhibition compared to other synthesized compounds. Generally, the presence of sulfur and nitrogen in the heterocyclic ligand skeleton shows diverse biological activities. Triazoles and tetrazoles are important heterocyclic compounds that show anticancer activity.[59,60] Incorporating two azole compounds in one structure (ligand) is new method to explore their anticancer activity beside their complex synthesis, which considered a challenge for inorganic chemists.

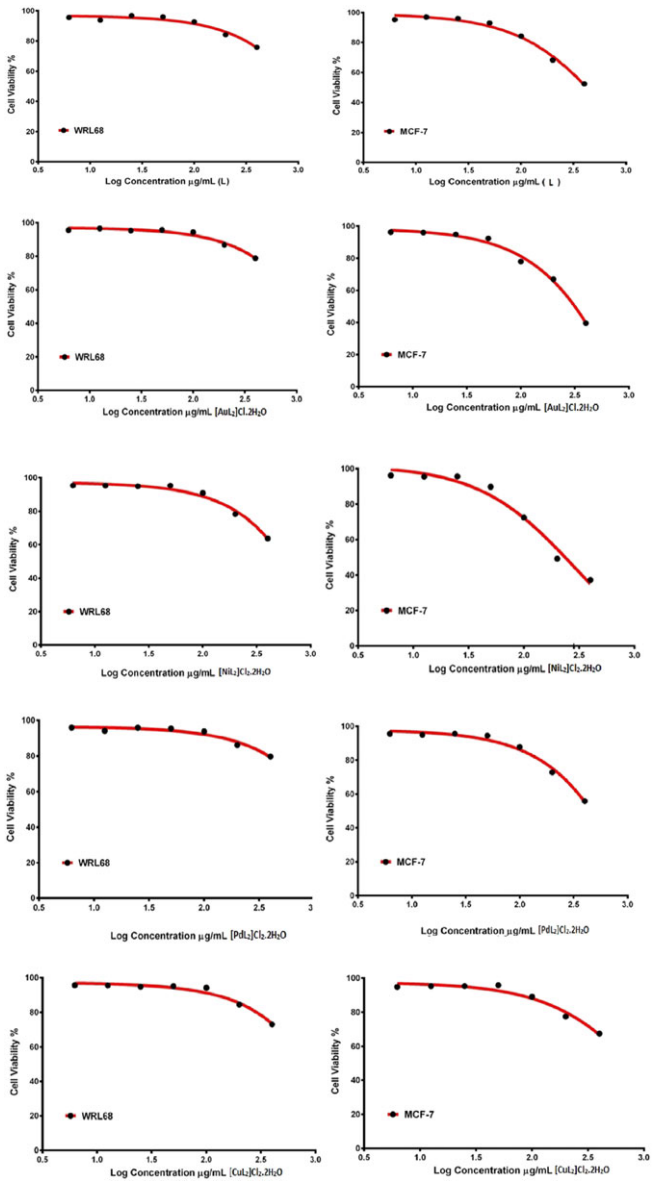

FIGURE 5 IC_{50} of the prepared ligand and its complexes in the normal WRL68 cell line and the cancer MCF-7 cell line

5 | CONCLUSIONS

In spite of ligands being multidentate with different donor atoms, the coordination was bidentate through two nitrogen atoms in their five-membered ring form. The complexes of gold, palladium, nickel, and copper have square planer shape with chemical formulas; $[AuL_2]Cl.2H_2O$, $[PdL_2]Cl_2.2H_2O$, $[NiL_2]Cl_2.2H_2O$, and $[CuL_2]$ respectively, all are chloride and hydrate salts except copper complex that was neutral and anhydrous (Figure 6). The MTT assay methods of selected compounds have shown significant cytotoxicity, the gold and nickel complexes have higher values against the MCF-7 cell line and their IC_{50} values are arranged as follows:

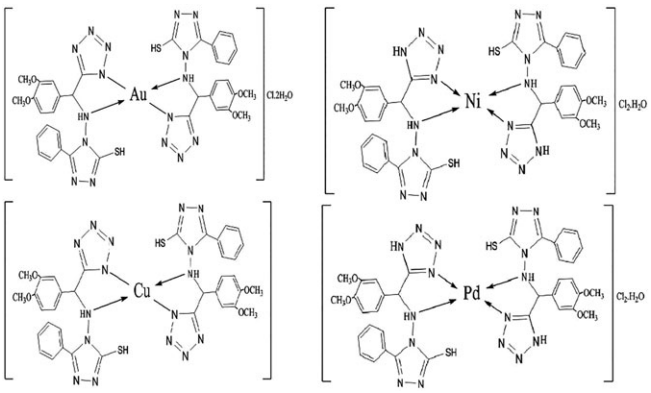

FIGURE 6 Suggested chemical structure of the prepared complexes

Au(III) < Ni(II) < L < Cu(II) < Pd(II). The high charge of gold (+3) could be of significance and may have played a role in the anticancer activity (Figure 6).

REFERENCES

[1] J. Ferlay, I. Soerjomataram, R. Dikshit, S. Eser, C. Mathers, M. Rebelo, D. Parkin, D. Forman, F. Bray, *Int. J. Cancer* **2015**, *136*, 359.

[2] M. Ghorab, M. Alsaid, M. Al-Dosari, *Acta Pol. Pharm.* **2016**, *73*, 1147.

[3] M. Arshad, A. Bhat, S. Pokharel, J. Kim, E. Lee, F. Athar, I. Choi, *Eur. J. Med. Chem.* **2014**, *71*, 229.

[4] F. Ahmed, A. Abd El-Hafeez, S. Abbas, D. Abdelhamid, M. Abdel-Aziz, *Eur. J. Med. Chem.* **2018**, *151*, 705.

[5] L. Al-Wahaibi, H. Abu-Melha, D. Ibrahim, *J. Chem.* **2018**, *2018*, 1.

[6] P. Kaur, A. Chawla, *Int. Res. J. Pharm.* **2017**, *8*, 10.

[7] V. Dhayanithi, S. Syed, K. Kumaran, K. Sankar, V. Ragavan, K. Goud, S. Kumari, H. Pati, *J. Serb. Chem. Soc.* **2011**, *76*, 165.

[8] W. El-Sayed, R. Abdel Megeid, H. Abbas, *Arch. Pharm. Res.* **2011**, *34*, 1085.

[9] N. Umarani, I. Kaliappan, N. Singh, *Pharma Chem.* **2010**, *2*, 159.

[10] U. Shankar, S. Jain, N. Sinha, N. Kishore, R. Chandra, S. Arora, *Eur. J. Med. Chem.* **2004**, *39*, 579.

[11] N. Jain, V. Pandey, *J. Chem. Chem. Sci.* **2018**, *8*, 693.

[12] A. Rajasekaran, P. Thampi, *Eur. J. Med. Chem.* **2005**, *40*, 1359.

[13] A. Rajasekaran, P. Thampi, *Eur. J. Med. Chem.* **2004**, *39*, 273.

[14] P. Lamie, J. Philoppes, A. Azouz, N. Safwat, *J. Enzyme Inhib. Med. Chem.* **2017**, *32*, 805.

[15] C. Kumar, D. Parida, A. Santhoshi, A. Kota, B. Sridhar, V. Rao, *MedChemComm* **2011**, *2*, 486.

[16] W. El-Sayed, S. El-Kosy, O. Ali, H. Emselm, A. Abdel-Rahman, *Acta Pol. Pharm.* **2012**, *69*, 669.

[17] M. Mphahlele, S. Gildenhuys, N. Parbhoo, *Molecules* **2017**, *22*, 1719.

[18] E. Popova, A. Protas, R. Trifonov, *Anticancer Agents Med Chem.* **2017**, *17*, 1856.

[19] H. Jonassen, J. Nelson, D. Schmitt, R. Henry, D. Moore, *Inorg. Chem.* **1970**, *9*, 2678.

[20] C. Orvig, M. Abrams, *Chem. Rev.* **1999**, *99*, 2201.

[21] B. Rosenberg, L. Vancamp, J. Trosko, V. Mansour, *Nature* **1969**, *222*, 385.

[22] D. Shaloam, P. Tchounwou, *Eur. J. Pharmacol.* **2014**, *40*, 364.

[23] L. Esteban, J. Cadavid-Vargas, A. Virgilio, S. Etcheverry, *Curr. Med. Chem.* **2017**, *24*, 112.

[24] W. Wani, U. Baig, S. Shreaz, R. Shiekh, P. Iqbal, E. Jameel, A. Ahmad, S. MohdSetapar, M. Mushtaque, L. Hun, *New J. Chem.* **2016**, *40*, 1063.

[25] V. Thamilarasan, N. Sengottuvelan, A. Sudha, P. Srinivasan, G. Chakkaravarthi, *J. Photochem. Photobiol. B* **2016**, *162*, 558.

[26] E. Jahromi, A. Divsalar, A. Saboury, S. Khaleghizadeh, H. Mansouri-Torshizi, I. Kostova, *J. Iran. Chem. Soc.* **2016**, 135, 967, *13*.

[27] Z. Chen, C. Orvig, H. Liang, *Curr. Top. Med. Chem.* **2017**, *17*, 3131.

[28] D. Bernard, *Anticancer Res* **2004**, *24*, 1529.

[29] N. Pantelić, B. Zmejkovski, D. Marković, J. Vujić, T. Stanojković, T. Sabo, G. Kaluđerović, *Metals* **2016**, *6*, 226.

[30] P. Calamai, S. Carotti, A. Guerri, L. Messori, E. Mini, P. Orioli, G. Speroni, *J. Inorg. Biochem.* **1997**, *66*, 103.

[31] T. Zou, C. Lum, S. Chui, C. Che, *Angew. Chem.* **2013**, *125*, 3002.

[32] R. Rubbiani, T. Zehnder, C. Mari, O. Blacque, K. Venkatesan, G. Gasser, *ChemMedChem* **2014**, *9*, 2781.

[33] N. Al-Masoudi, B. Abdullah, A. Ess, R. Loddo, P. LaColla, *Arch. Pharm.* **2010**, *343*, 222.

[34] L. Tušek-Božić, I. Matijašić, G. Bocelli, P. Sgarabotto, A. Furlani, V. Scarcia, A. Papaioannou, *Inorg. Chim. Acta* **1991**, *185*, 229.

[35] M. Malik, O. Dar, P. Gull, M. Wani, A. Hashmi, *MedChemComm.* **2018**, *9*, 409.

[36] S. Lee, A. Hille, C. Frias, B. Kater, B. Bonitzki, S. Wölfl, H. Scheffler, A. Prokop, R. Gust, *J. Med. Chem.* **2010**, *53*, 6064.

[37] P. Kalaivani, S. Saranya, P. Poornima, R. Prabhakaran, F. Dallemer, V. Padma, K. Natarajan, *Eur. J. Med. Chem.* **2014**, *82*, 584.

[38] F. Andrew, P. Ajibade, *J. Coord. Chem.* **2018**, *71*, 16.

[39] A. Saha, R. Kumar, R. Kumar, C. Devakumar, *Indian J. Chem.* **2010**, *4*, 526.

[40] L. Yadav, *Organic Spectroscopy*, Springer Science & Business Media, Dordrecht **2013**.

[41] S. Jubie, P. Sikdar, S. Antony, R. Kalirajan, B. Gowramma, S. Gomathy, K. Elango, *Pak. J. Pharm. Sci.* **2011**, *24*, 109.

[42] P. Larkin, *Infrared and Raman Spectroscopy: Principles and Spectral Interpretation*, Elsevier Inc, Amsterdam, Netherlands **2018**.

[43] A. J. Alabdali, *J. Appl. Chem.* **2012**, *3*, 5.

[44] U. Holzgrabe, *NMR Spectroscopy in Pharmaceutical Analysis*, Elsevier LTD, Amsterdam, Netherlands **2017**.

[45] V. Zhdankin, C. Kuehl, A. Krasutsky, J. Bolz, B. Mismash, J. Woodward, A. Simonsen, *Tetrahedron Lett.* **1995**, *36*, 7975.

[46] G. Levy, R. Lichter, G. Nelson, *Carbon-13 Nuclear Magnetic Resonance Spectroscopy*, Krieger Publishing Company, Malabar, FL, USA **1992**.

[47] F. Martak, A. Wahyudi, I. Candrawati, M. Nur, F. Lestari, *Pharm. Chem. J.* **2017**, *4*, 61.

[48] F. Scheinmann Ed., *An Introduction to Spectroscopic Methods for the Identification of Organic Compounds: Mass Spectrometry, Ultraviolet Spectroscopy, Electron Spin Resonance Spectroscopy, Nuclear Magnetic Resonance Spectroscopy (Recent Developments), Use of Various Spectral Methods Together, and Documentation of Molecular Spectra*, Elsevier, Pergamon, **1973**.

[49] P. Byabartta, *Afri. J. Pure Appl. Chem.* **2009**, *3*, 177.

[50] C. jorgenson, *Absorption Spectra and Chemical Bondind in Complexes*; Pergamon press, Oxford, UK **1962**.

[51] B. figgis, *Introduction to Ligand Field*, Inerscience, New York, NY **1966**.

[52] S. Shupack, E. Billig, R. Clark, R. Williams, H. Gray, *J. Am. Chem. Soc.* **1964**, *86*, 4594.

[53] B. Bosnich, *J. Am. Chem. Soc.* **1968**, *90*, 627.

[54] E. Sekhar, K. Jayaveera, S. Srihari, *IOSR J. Appl. Chem.* **2015**, *8*, 2278.

[55] R. Rush, D. Jr, R. Le Grand, *Inorg. Chem.* **1975**, *14*, 2543.

[56] J. Inba, B. Annaraj, S. Thalamuthu, M. Neelakantan, *Bioinorg. Chem. Appl.* **2013**, *2013*, 439848.

[57] I. Ali, W. Wani, K. Saleem, *Synth. React. Inorg. Metal-Org. Nano-Met. Chem.* **2013**, *43*, 1162.
[58] M. Berridge, P. Herst, A. Tan, *Biotechnol. Annu. Rev.* **2005**, *11*, 127.
[59] M. Gilandoust, K. Harsha, C. Mohan, A. Raquib, S. Rangappa, V. Pandey, P. Lobie, K. Rangappa, *Bioorg. Med. Chem. Lett.* **2314**, *28*, 2018.
[60] S. Gorle, S. Maddila, S. Maddila, K. Naicker, M. Singh, P. Singh, S. Jonnalagadda, *Anticancer Agents Med Chem.* **2017**, *17*, 464.

How to cite this article: Abdnoor ZM, Alabdali AJ. Synthesis, characterization, and anticancer activity of some azole-heterocyclic complexes with gold(III), palladium(II), nickel(II), and copper(II) metal ions. *J Chin Chem Soc*. 2019;1–10. https://doi.org/10.1002/jccs.201900010